

# Expansion dynamics of a cylindrical-shell-shaped strongly dipolar condensate

Luis E. Young-S.<sup>a</sup>, S. K. Adhikari<sup>b</sup>

<sup>a</sup>*Grupo de Modelado Computacional, Facultad de Ciencias Exactas y Naturales, Universidad de Cartagena, 130015 Cartagena de Indias, Bolívar, Colombia*

<sup>b</sup>*Instituto de Física Teórica, UNESP - Universidade Estadual Paulista, 01.140-070 São Paulo, São Paulo, Brazil*

---

## Abstract

A Bose-Einstein condensate (BEC) formed on a curved surface with a distinct topology has been a hot topic of intense research, in search of new phenomena in quantum physics as well as for its possible application in quantum computing. In addition to the study of a spherical-shell-shaped BEC, we studied the formation of a cylindrical-shell-shaped harmonically-trapped dipolar BEC of  $^{164}\text{Dy}$  atoms theoretically using an improved mean-field model including a Lee-Huang-Yang-type interaction, meant to stop a collapse at high atom density. To test the robustness of the cylindrical-shell-shaped BEC, here we study its expansion in the same model. We find that as the harmonic trap in the  $x$  and  $y$  directions are removed, maintaining the axial trap, the cylindrical-shell-shaped BEC expands in the  $x$ - $y$  plane without deformation, maintaining its shell-shaped structure. After an adequate radial expansion, the axial trap can be relaxed for a desired axial expansion of the cylindrical-shell-shaped BEC allowing its observation.

---

## 1. Introduction

A Bose-Einstein condensate (BEC) of bosonic atoms has been fundamental in investigating different quantum phenomena, which, although previously predicted and studied theoretically, could not be realized experimentally otherwise. For example, to mention a few, a rotating BEC has generated a very large vortex lattice confirming its superfluidity [1]; quantum phase transition has been realized in a BEC on an optical lattice [2, 3]; bright matter-wave solitons have been studied in a quasi-one-dimensional attractive BEC [4, 5]; the effect of spin-orbit coupling of neutral atoms on a spinor BEC has been investigated [6]; a quasi-two-dimensional (quasi-2D) supersolid BEC has been studied experimentally [7, 8]. Most of these studies were performed in the three-dimensional (3D) Euclidean space with trivial topology. Nevertheless, new physics is expected to emerge on curved surfaces with distinct topology, for example, on the surface of a hollow sphere [9, 10, 11, 12] or a hollow cylinder [13], the latter, although topologically equivalent to a toroid or a ring, has a distinct geometrical shape. Generation of vortices on a curved surface is distinct from the same in a 3D space [14, 15, 16]. Unique superfluid properties

may exist in a BEC in a toroidal trap with distinct topology [17, 18, 19]. Moreover, quantum states with distinct topology [20, 21, 22, 23] may have useful application in the field of quantum computing [24].

In view of the above-mentioned interests in a BEC with a distinct topology, experimental activity has started to create and study a BEC formed on a spherical surface in the form of a spherical bubble. In the presence of gravity, even in a spherical-shell-shaped trap, this is not possible to create a spherical bubble-shaped BEC, as gravity will bring down the atoms from the top of the bubble making a hole. However, partially circumventing this problem, a hemispherical-shell-shaped BEC of  $^{87}\text{Rb}$  atoms has been created in a laboratory on earth [25] by a gravity compensation mechanism. As a first step to create a BEC in a spherical-shell-shaped trap, a spherical bubble of ultracold  $^{87}\text{Rb}$  atoms in orbital microgravity [9] in an orbiting space station, without the effect of gravity, has been realized [10, 11, 12] following a suggestion [26, 27] and studies in Ref. [28, 29, 30, 31]. Following another theoretical suggestion [32, 33] and related investigations [34, 35, 36, 37], a binary BEC of  $^{23}\text{Na}$  and  $^{87}\text{Rb}$  atoms have been observed in a laboratory on earth [38], in the presence of gravity, with the  $^{23}\text{Na}$  atoms forming a spherical bubble surrounding a solid spherical core of  $^{87}\text{Rb}$  atoms. These experiments [9, 25, 38] for the creation of a BEC with a distinct topology in the form of a spherical bubble re-

---

*Email addresses:* lyoung@unicartagena.edu.co (Luis E. Young-S.), sk.adhikari@unesp.br (S. K. Adhikari)

quire a complex manipulation of external conditions or of the confining trap.

Recently, we have demonstrated [13] the possibility of the formation of a cylindrical-shell-shaped BEC of strongly dipolar  $^{164}\text{Dy}$  atoms, with distinct topology, in a *harmonic* trap, not requiring a cylindrical-shell-shaped trap. Although a cylindrical shell is topologically equivalent to a circular ring, it has a different geometric shape. This may allow the possibility of the study of new physics on the surface of a cylinder, like the creation of vortex or vortex lattice. In this paper we test the robustness of these cylindrical-shell-shaped states by real-time propagation during an expansion for a long period of time. We demonstrate that the cylindrical-shell-shaped state expands without destroying the topology to a very large size, where it can be photographed and its presence be experimentally confirmed. For the detection of a shell-shaped BEC, its expansion dynamics is of utmost importance as emphasized in different studies in the context of a spherical-shell-shaped state [38, 39, 40, 41].

The theoretical investigation of this paper will be based on an improved mean-field model including a Lee-Huang-Yang-type (LHY) interaction [42], appropriately modified for dipolar atoms [43, 44, 45]. In a mean-field Gross-Pitaevskii (GP) model with cubic nonlinearity, a strongly dipolar BEC collapses [46, 47], and the inclusion of a repulsive LHY interaction [43, 45] in theoretical investigations stabilizes a strongly dipolar condensate [48] to form a droplet [46, 47, 49] in a strong harmonic trap. For a large number of strongly dipolar atoms, in a strong quasi-2D harmonic trap, a spatially-periodic [8] triangular- [8, 46, 47], square- [50], or honeycomb-lattice [50] structure of droplets or a labyrinthine state [51] could be formed. The present cylindrical-shell-shaped  $^{164}\text{Dy}$  BEC is formed in a strong three-dimensional harmonic trap, and not a quasi-2D trap. As the number of atoms is increased beyond a critical value, the dipolar atoms are deposited on the outer surface of a hollow cylinder, for scattering length  $a$  in the range  $85a_0 \gtrsim a \gtrsim 80a_0$  [13], where  $a_0$  is the Bohr radius. For the cylindrical-shell-shaped states to appear, the number of atoms  $N$  should be in the range  $250000 \gtrsim N \gtrsim 150000$ , the trap frequency  $f_z$  along the polarization  $z$  direction in the range  $250 \text{ Hz} \gtrsim f_z \gtrsim 150 \text{ Hz}$  and those in the transverse  $x$ - $y$  plane are taken as  $f_x, f_y \approx 0.75f_z$  [13]. If the confining harmonic trap in the  $x$ - $y$  plane is made slightly anisotropic ( $f_x \neq f_y$ ), the cylindrical shell of the strongly dipolar BEC becomes elliptical in nature. These strongly dipolar BECs have a large number of atoms, not trivial for experimental realization [52], specially in the overall attractive regime

due to large atom loss by three-body interaction. A way to optimize the observation of strongly dipolar BECs with a large number of atoms ( $N > 2 \times 10^5$ ), appropriate for the study of the present cylindrical-shell-shaped BECs, has recently appeared in the literature [53].

The expansion of a cylindrical-shell-shaped BEC of circular or elliptic section can be considered as a two-step process. First, we consider its quasi-free expansion by setting the transverse trap frequencies to zero ( $f_x = f_y = 0$ ), but maintaining the frequency in the polarization direction  $f_z$  unchanged, employing real-time propagation. We find that the initial symmetry of the cylindrical-shell-shaped BEC is maintained during the quasi-free expansion. In this case, as the radius of the cylindrical shell increases during this expansion, the length of the cylinder (along the  $z$  direction) reduces. The reduction of the root-mean-square (rms) size in the  $z$  direction is accompanied by a periodic oscillation, controlled by the frequency of the trap in the  $z$  direction, in agreement with a theoretical prediction [54]. After an adequate radial expansion, the axial  $z$  frequency of the trap  $f_z$  can be reduced slightly for an axial expansion of the system along  $z$  direction to a desirable size to be observed experimentally. We verified that the  $z$  length increases without destroying the cylindrical-shell-shaped structure of the BEC (not elaborated in this paper).

The expansion dynamics of the present cylindrical-shell-shaped strongly dipolar BEC is very different from the free expansion of a spherical-shell-shaped nondipolar BEC. In the latter case, unlike in the present case, the BEC expands inwards and outwards thus filling in the entire space destroying the shell-shaped structure very quickly [39]. The same may happen in the case of a freely expanding nondipolar ring-shaped BEC [55] or a freely expanding dipolar toroid-shaped BEC [56] with the same topology as the present cylindrical-shell-shaped BEC. The ring-shaped BEC again expands both inwards and outwards closing the hole in the ring entirely, thus destroying ring-shaped structure. This sets a limitation on the direct experimental observation of a spherical-shell-shaped nondipolar BEC. There have been suggestions about how to maintain the spherical-shell-shaped structure using a binary BEC [32, 33, 38] or employing matter-wave lensing techniques [40]. The strong long-range dipolar repulsion between atoms located at diagonally opposite positions in the same  $x$ - $y$  plane in the present cylindrical-shell-shaped-state stops the inward expansion, thus stabilizing the shell structure.

In Sec. II we present the improved mean-field model including the LHY interaction and reduce it to a dimensionless form. In addition, we provide an expression

of the dimensionless energy functional of the system (energy per atom.) In Sec. III we present our numerical results for trap frequency  $f_z = 167$  Hz. This axial trap frequency was recently used in the study of a strongly dipolar  $^{164}\text{Dy}$  BEC [8, 57]. In addition to presenting the profile of the hollow cylindrical shape of the quasi-freely expanding shell-shaped  $^{164}\text{Dy}$  BEC, we also present the evolution of energy and axial and radial sizes of the expanding BEC. In Sec. IV we present a brief summary of our findings.

## 2. Improved mean-field model

We consider a dipolar BEC of  $N$   $^{164}\text{Dy}$  atoms, polarized along the  $z$  direction, of mass  $m$  each, and with atomic scattering length  $a$ . The magnetic dipolar interaction between two dipolar atoms, of magnetic moment  $\mu$  each, located at  $\mathbf{r} \equiv \{\mathbf{x}, \mathbf{y}, \mathbf{z}\}$  and  $\mathbf{r}' \equiv \{\mathbf{x}', \mathbf{y}', \mathbf{z}'\}$  is

$$U_{\text{dd}}(\mathbf{R}) = \frac{\mu_0\mu^2}{4\pi} \frac{1 - 3\cos^2\theta}{|\mathbf{R}|^3} \equiv \frac{3\hbar^2 a_{\text{dd}}}{m} \frac{1 - 3\cos^2\theta}{|\mathbf{R}|^3}, \quad (1)$$

where  $\theta$  is the angle made by the vector  $\mathbf{R} \equiv \mathbf{r} - \mathbf{r}'$  with the polarization  $z$  direction,  $\mu_0$  is the permeability of vacuum, and the dipolar length  $a_{\text{dd}} = \mu_0\mu^2 m / (12\pi\hbar^2)$  is a measure of the strength of dipolar interaction, whereas the scattering length  $a$  is a measure of the strength of contact interaction.

The statics and dynamics of a cylindrical-shell-shaped BEC [13] is governed by the following improved mean-field Gross-Pitaevskii equation with the inclusion of the dipolar and the LHY interaction [58, 59, 60, 61]

$$i\hbar \frac{\partial\psi(\mathbf{r}, t)}{\partial t} = \left[ -\frac{\hbar^2}{2m} \nabla^2 + U(\mathbf{r}) + \frac{4\pi\hbar^2}{m} aN |\psi(\mathbf{r}, t)|^2 + \frac{3\hbar^2}{m} a_{\text{dd}} N \int U_{\text{dd}}(\mathbf{R}) |\psi(\mathbf{r}', t)|^2 d\mathbf{r}' + \frac{\gamma_{\text{LHY}} \hbar^2}{m} N^{3/2} |\psi(\mathbf{r}, t)|^3 \right] \psi(\mathbf{r}, t), \quad (2)$$

$$U(\mathbf{r}) = \frac{1}{2} m (\omega_x^2 x^2 + \omega_y^2 y^2 + \omega_z^2 z^2), \quad (3)$$

where  $\omega_x (\equiv 2\pi f_x)$ ,  $\omega_y (\equiv 2\pi f_y)$ ,  $\omega_z (\equiv 2\pi f_z)$  are the angular frequencies of the harmonic trap (3) along  $x, y, z$  directions, respectively. The axis of the cylindrical shell is aligned along the polarization  $z$  direction of dipolar atoms. The wave function  $\psi(\mathbf{r}, t)$  at time  $t$  is normalized as  $\int |\psi(\mathbf{r}, t)|^2 d\mathbf{r} = 1$ . The strength of LHY interaction  $\gamma_{\text{LHY}}$  is given by [43, 44, 45]

$$\gamma_{\text{LHY}} = \frac{128}{3} \sqrt{\pi a^5} Q_5(\varepsilon_{\text{dd}}), \quad \varepsilon_{\text{dd}} = \frac{a_{\text{dd}}}{a}, \quad (4)$$

where the auxiliary function  $Q_5(\varepsilon_{\text{dd}})$  includes the correction to the LHY interaction [42] due to the dipolar interaction and is given by [44]

$$Q_5(\varepsilon_{\text{dd}}) = (1 - \varepsilon_{\text{dd}})^{5/2} {}_2F_1\left(-\frac{5}{2}, \frac{1}{2}; \frac{3}{2}; \frac{3\varepsilon_{\text{dd}}}{\varepsilon_{\text{dd}} - 1}\right), \quad (5)$$

where  ${}_2F_1$  is the hypergeometric function [62]. Using an integral representation of this function [62], the auxiliary function  $Q_5$  can be written as [59]

$$Q_5(\varepsilon_{\text{dd}}) = \int_0^1 dx (1 - \varepsilon_{\text{dd}} + 3x^2 \varepsilon_{\text{dd}})^{5/2}, \quad (6)$$

$$= \frac{(3\varepsilon_{\text{dd}})^{5/2}}{48} \Re \left[ (8 + 26\eta + 33\eta^2) \sqrt{1 + \eta} + 15\eta^3 \ln \left( \frac{1 + \sqrt{1 + \eta}}{\sqrt{\eta}} \right) \right], \quad \eta = \frac{1 - \varepsilon_{\text{dd}}}{3\varepsilon_{\text{dd}}}, \quad (7)$$

where  $\Re$  denotes the real part. The dimensionless ratio  $\varepsilon_{\text{dd}}$ , viz. Eq. (4), determines the strength of dipolar interaction relative to that of contact interaction and is useful to classify and study many properties of a dipolar BEC. In the present study of a strongly dipolar BEC  $\varepsilon_{\text{dd}} > 1$ , while  $Q_5(\varepsilon_{\text{dd}})$  of Eqs. (6) and (7) are complex with a small imaginary part and a much larger real part [63]. The imaginary part contributes to a loss of atoms from the BEC and will be neglected as in all other investigations [50, 64, 65, 66, 67]. In this study we will use Eq. (7) in our numerical calculation.

It is convenient to present Eq. (2) in the following dimensionless form by scaling lengths in terms of  $l = \sqrt{\hbar/m\omega_z}$ , time in units of  $t_0 \equiv \omega_z^{-1}$ , angular frequency in units of  $\omega_z$ , energy in units of  $\hbar\omega_z$  and density  $|\psi|^2$  in units of  $l^{-3}$

$$i \frac{\partial\psi(\mathbf{r}, t)}{\partial t} = \left[ -\frac{1}{2} \nabla^2 + \frac{1}{2} (f_x^2 x^2 + f_y^2 y^2 + z^2) + 4\pi a N |\psi(\mathbf{r}, t)|^2 + 3a_{\text{dd}} N \int U_{\text{dd}}(\mathbf{R}) |\psi(\mathbf{r}', t)|^2 d\mathbf{r}' + \gamma_{\text{LHY}} N^{3/2} |\psi(\mathbf{r}, t)|^3 \right] \psi(\mathbf{r}, t), \quad (8)$$

where all variables are scaled. We will use the same symbols to represent the scaled and unscaled variables without any risk of confusion.

The dimensionless improved mean-field GP equation (8) can be derived from the following variational principle

$$i \frac{\partial\psi}{\partial t} = \frac{\delta E}{\delta\psi^*}, \quad (9)$$

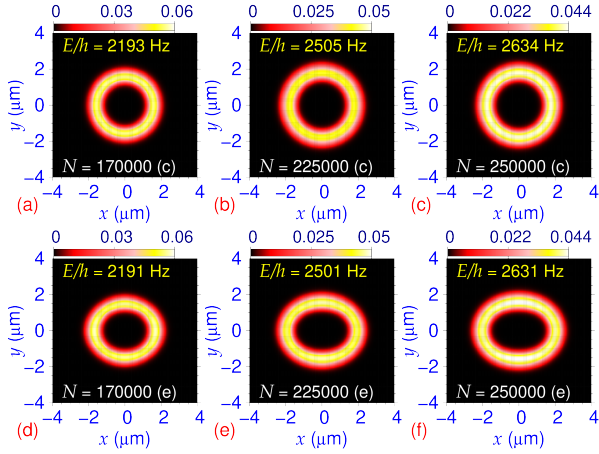


Figure 1: Contour plot of dimensionless 2D density  $n_{2D}(x, y)$  of  $^{164}\text{Dy}$  atoms of cylindrical-shell-shaped states for (a) and (d)  $N = 170000$ , (b) and (e)  $N = 225000$ , (c) and (f)  $N = 250000$ . In all cases  $f_z = 167$  Hz, in (a)-(c)  $f_x = f_y = 0.75f_z$ , establishing three systems with circular (ci) section and in (d)-(f)  $f_x = 120$  Hz and  $f_y = 130$  Hz for three states with elliptic (el) section. The corresponding energies per atom  $E$  (in units of  $h$ ) are shown in the inset of each plot.

where the energy functional  $E$  given by

$$\begin{aligned}
 E = & \frac{1}{2} \int d\mathbf{r} [|\nabla\psi(\mathbf{r})|^2 + (f_x^2 x^2 + f_y^2 y^2 + z^2)|\psi(\mathbf{r})|^2 \\
 & + 3a_{\text{dd}}N|\psi(\mathbf{r})|^2 \int U_{\text{dd}}(\mathbf{R})|\psi(\mathbf{r}')|^2 d\mathbf{r}' \\
 & + 4\pi Na|\psi(\mathbf{r})|^4 + \frac{4\gamma_{\text{LHY}}}{5}N^{3/2}|\psi(\mathbf{r})|^5] \quad (10)
 \end{aligned}$$

is the energy per atom of a stationary state.

### 3. Numerical Results

To study the expansion dynamics of a cylindrical-shell-shaped dipolar BEC of  $^{164}\text{Dy}$  atoms, the partial differential GP equation (8) is solved, numerically, using FORTRAN or C programs [60] or specially their open-multiprocessing counterparts [68, 69]. We employ the split-time-step Crank-Nicolson method by real-time propagation [70] using the converged wave function obtained by imaginary-time propagation as the initial state. It is numerically difficult to deal with the divergent  $1/|\mathbf{R}|^3$  term in the dipolar potential (1) in configuration space. To overcome this difficulty, we evaluate the integral over the long-range dipolar potential in the improved mean-field model (8) by a Fourier transformation to momentum space. In this fashion, after solving the problem in momentum space, the configuration space solution is obtained by a backward Fourier transformation [60].

Although,  $a_{\text{dd}} = 130.8a_0$  for  $^{164}\text{Dy}$  atoms, we have a certain flexibility in fixing the scattering length  $a$ , as the scattering length can be modified employing the Feshbach resonance [71] technique by manipulating an external electromagnetic field. In this study, as in Ref. [13], we take the scattering length  $a = 80a_0$ . The experimental estimate of the scattering length,  $a = (92 \pm 8)a_0$  [72], leads to a much stronger contact repulsion and does not allow the formation of a cylindrical-shell-shaped BEC. With the reduction of contact repulsion, the present choice of scattering length ( $a = 80a_0$ ) facilitates the formation of a pronounced cylindrical-shell-shaped BEC.

In this study of cylindrical-shell-shaped states in a strongly dipolar BEC of  $^{164}\text{Dy}$  atoms, we will consider the axial trap frequency  $f_z = 167$  Hz, which is the same used in the pioneering experiments on 2D hexagonal supersolid formation with  $^{164}\text{Dy}$  atoms [8, 57] and also used in some theoretical investigations [13, 50, 67]. It is true that the frequency  $f_z$  is the same in both cases, but the quasi-2D trap of Refs. [8, 57] ( $f_z \gg f_x, f_y$ ) is very different from the trap in the present study ( $f_x, f_y = 0.75f_z$ ) with much larger trap frequencies along the  $x$  and  $y$  directions. Cylindrical-shell-shaped states are formed for  $f_z \gtrsim 150$  Hz; however, for larger  $f_z$  the inner radius of the cylindrical shell gradually reduces and eventually solid cylindrical states are formed for  $f_z \gtrsim 275$  Hz. On the other hand, for smaller  $f_z$  ( $f_z \lesssim 150$ ) four droplet-states are preferentially formed. This is why in this study we will consider only  $f_z = 167$  Hz, where pronounced hollow cylindrical states with thin shell and large internal radius are formed. For  $m(^{164}\text{Dy})$  atoms with mass  $\approx 164 \times 1.66054 \times 10^{-27}$  kg,  $\hbar = 1.0545718 \times 10^{-34}$  m<sup>2</sup> kg/s, and for  $f_z = 167$  Hz, the unit of length is  $l = \sqrt{\hbar/(2\pi m f_z)} = 0.6075 \mu\text{m}$ , the unit of time  $t_0 \equiv (2\pi \times f_z)^{-1} = 0.953$  ms.

A cylindrical-shell-shaped state is best illustrated through the integrated 2D density  $n_{2D}(x, y)$  defined by an axial  $z$  integration over density

$$n_{2D}(x, y) = \int_{-\infty}^{\infty} dz |\psi(x, y, z)|^2. \quad (11)$$

A contour plot of the 2D density  $n_{2D}(x, y)$  of a few cylindrical-shell-shaped states with circular (ci) and elliptic (el) sections in a dipolar BEC of  $^{164}\text{Dy}$  atoms is considered next for  $a = 80a_0, f_z = 167$  Hz. In Fig. 1, we display a contour plot of the 2D density  $n_{2D}(x, y)$  of a cylindrical-shell-shaped state with circular section for (a)  $N = 170000$ , (b)  $N = 200000$  and (c)  $N = 225000$  and  $f_x = f_y = 0.75f_z$ . Next we display the same with elliptic section for (d)  $N = 170000$ , (e)  $N = 225000$  and (f)  $N = 250000$  and  $f_x = 120$  Hz and  $f_y = 130$

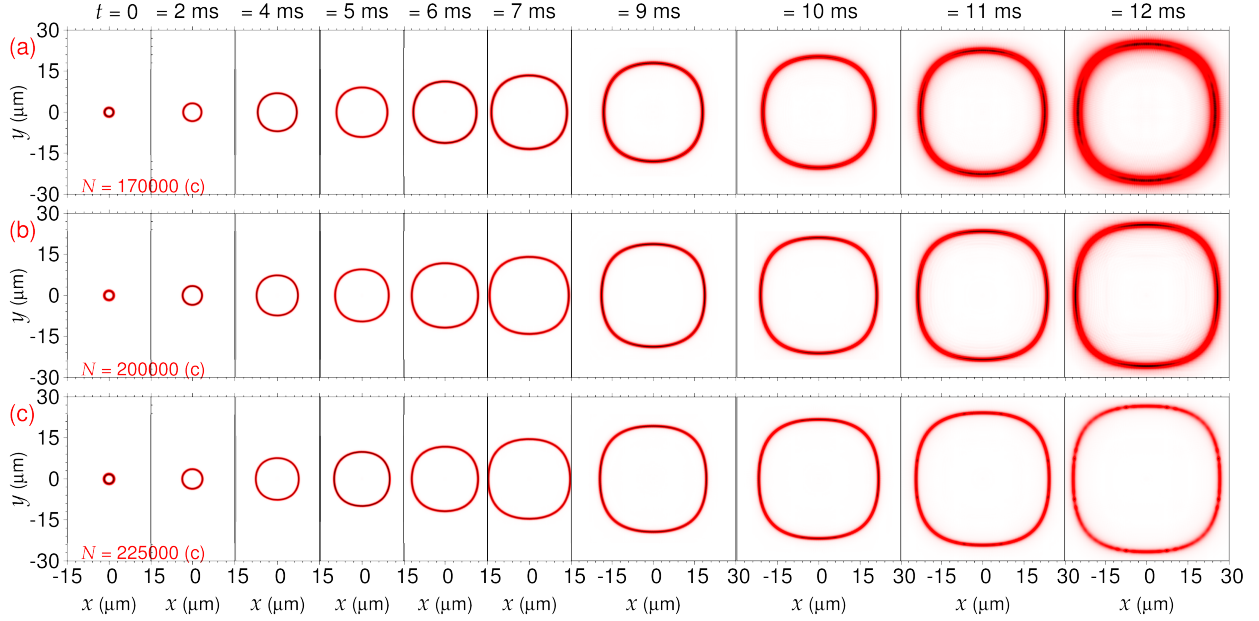


Figure 2: Profile of the cylindrical-shell-shaped strongly dipolar  $^{164}\text{Dy}$  BEC with circular section during quasi-free expansion at times  $t = 0, 2$  ms, 4 ms, 5 ms, 6 ms, 7 ms, 9 ms, 10 ms, 11 ms, 12 ms, through a contour plot of the quasi-2D density  $n_{2D}(x, y)$  for (a)  $N = 170000$  (top panel), (b)  $N = 200000$  (middle panel), and (c)  $N = 225000$  (bottom panel). The dynamics is studied by real-time propagation, with the axial trap  $f_z = 167$  Hz and radial traps  $f_x = f_y = 0$ , using the appropriately trapped ( $f_z = 167$  Hz,  $f_x = f_y = 0.75f_z$ ) converged imaginary-time solution as the initial state at  $t = 0$ .

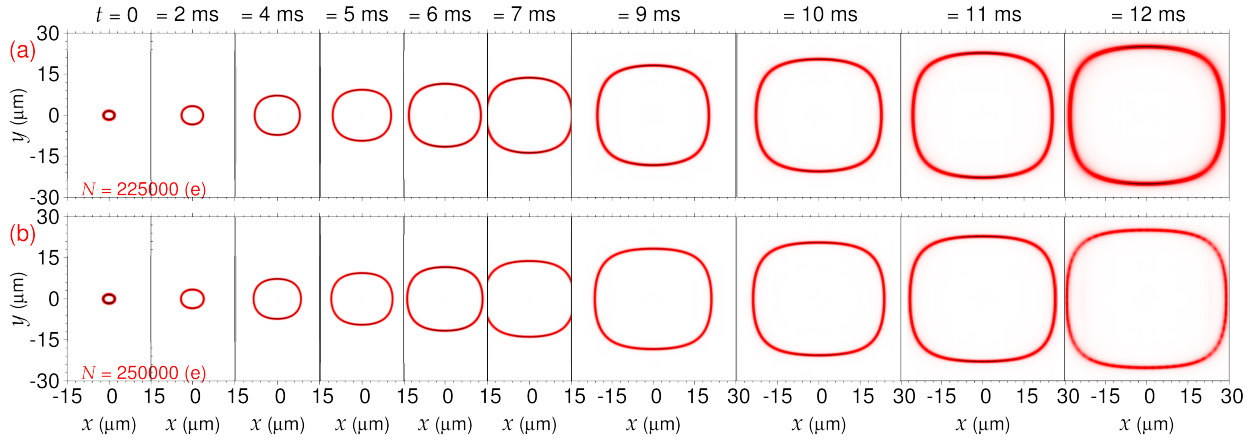


Figure 3: Profile of the cylindrical-shell-shaped strongly dipolar  $^{164}\text{Dy}$  BEC with elliptic section during quasi-free expansion at times  $t = 0, 2$  ms, 4 ms, 5 ms, 6 ms, 7 ms, 9 ms, 10 ms, 11 ms, 12 ms, through a contour plot of the quasi-2D density  $n_{2D}(x, y)$  for (a)  $N = 225000$  (top panel) and (b)  $N = 250000$  (bottom panel). The dynamics is studied by real-time propagation, with the axial trap  $f_z = 167$  Hz and the radial traps  $f_x = f_y = 0$ , using the appropriately trapped ( $f_x = 120$  Hz,  $f_y = 130$  Hz) converged imaginary-time solution as the initial state at  $t = 0$ .

Hz. The trap in plots 1(a)-(c) is cylindrically symmetric whereas this symmetry of the trap is broken in plots 1(d)-(f). Consequently, we find cylindrical-shell-shaped states in plots 1(a)-(c) with circular section and in plots 1(d)-(f) with elliptic section. In all cases the inner radius of the cylindrical shell is quite sharp and pronounced. The corresponding energies, given in the insets of the plots, of the elliptical cylinders are slightly smaller than those of the circular cylinders.

In a typical experiment, the cylindrical-shell-shaped state would be confirmed after an expansion to a detectable size by a two-step process. We study by real-time propagation a quasi-free expansion in the  $x$ - $y$  plane, by making  $f_x = f_y = 0$  at  $t = 0$ , while we maintain the BEC trapped along the  $z$  direction. As the cylindrical shape appears in the  $x$ - $y$  plane, such a quasi-free expansion in this plane is appropriate for our purpose. After a quasi-free expansion in the  $x$ - $y$  plane, the frequency of the trap in the  $z$  direction should be reduced/relaxed a bit for the cylindrical-shell-shaped state to expand in the  $z$  direction up to a desired size to visualize (not elaborated in this paper). In a fully free expansion ( $f_x = f_y = f_z = 0$ ) from the beginning, the cylindrical-shell-shaped BEC expands more in the  $z$  direction. As the intention is to have a large curved surface after expansion, this two-step process is more appropriate.

The quasi-free expansion dynamics as obtained by real-time propagation is presented in Fig. 2 for the cylindrical-shell-shaped states with circular section for (a)  $N = 170000$ , (b)  $N = 200000$ , and (c)  $N = 225000$   $^{164}\text{Dy}$  atoms through a contour plot of the 2D density  $n_{2D}(x, y)$  at times  $t = 0, 2$  ms, 4 ms, 5 ms, 6 ms, 7 ms, 9 ms, 10 ms, 11 ms, and 12 ms. The typical diameter of the cylindrical-shell-shaped state has increased from about  $4 \mu\text{m}$  to  $60 \mu\text{m}$  in 12 ms which will guaranty the observability of these states. The thickness of the cylindrical shell has increased a bit for  $N = 170000$ , although the internal hollow region is very prominent. With the increase of the number of atoms, after expansion, the cylindrical shell remains thin and sharp, viz. the bottom panel in Fig. 2 for  $N = 225000$ .

Next we study the quasi-free expansion of a cylindrical-shell-shaped state with elliptic section. We display in Fig. 3 this expansion dynamics of (a)  $N = 225000$  and (b)  $N = 250000$   $^{164}\text{Dy}$  atoms through a contour plot of the 2D density  $n_{2D}(x, y)$  at times  $t = 0, 2$  ms, 4 ms, 5 ms, 6 ms, 7 ms, 9 ms, 10 ms, 11 ms, and 12 ms. The sharpness of the shell structure after expansion in both cases in Fig. 3 are quite similar and is very pronounced. The expansion of the cylindrical-shell-shaped states in Fig. 3 is comparable to the same

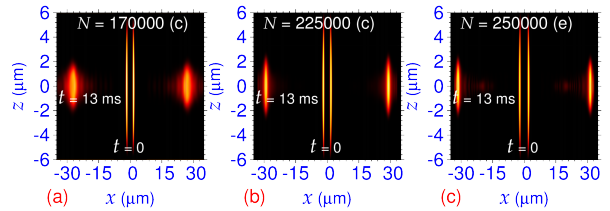


Figure 4: Contour plot of density  $|\psi(x, 0, z)|^2$  of the quasi-freely expanding cylindrical-shell-shaped dipolar BEC of  $^{164}\text{Dy}$  atoms at times  $t = 0$  (central region with small  $|x|$ ) and  $t = 13$  ms (outer region with large  $|x|$ ) for (a)  $N = 170000$ , (b)  $N = 225000$ , and (c)  $N = 250000$ . In (a) and (b) the section is circular (ci) corresponding to the expansion dynamics of Figs. 2(a) and (c), and in (c) the section is elliptic (el) corresponding to the expansion dynamics of Fig. 3(c).

in Fig. 2. The pronounced shell structure in Figs. 2 and 3 are due to the robustness of these states with strong dipolar interaction. The dipolar repulsion between the  $^{164}\text{Dy}$  atoms in the same  $x$ - $y$  plane and the dipolar attraction between the atoms in different  $x$ - $y$  planes make the robust cylindrical-shell-shaped states. The same will not be possible in the absence of a dipolar interaction. This is why the expansion of a nondipolar repulsive spherical-shell-shaped BEC [39] or a ring-shaped BEC [55] may easily destroy the internal hollow region.

The extended hollow region of the cylindrical-shell-shaped state is best illustrated through a contour plot of density  $|\psi(x, 0, z)|^2$  of the quasi-freely expanding cylindrical-shell-shaped dipolar BEC of  $^{164}\text{Dy}$  atoms at  $t = 0$  and at  $t = 13$  ms. This is displayed in Fig. 4 for (a)  $N = 170000$ , (b)  $N = 225000$  of a cylindrical-shell-shaped BEC of circular section, viz. Figs. 2(a) and (c), and in Fig. 4 for (c)  $N = 250000$  of a cylindrical-shell-shaped BEC of elliptic section, viz. Fig. 3(b). In all these plots the long and thin  $y = 0$  section of the cylinder at  $t = 0$  can be seen in the central region of small  $|x|$  values, whereas in the outer large  $|x|$  region, the short and wide section of the cylinder at  $t = 13$  ms can be seen. For larger  $N$  in Figs. 4(b) and (c), for  $N = 225000$  and  $N = 250000$ , the hollow cylinder remains sharp with thin wall, whereas the same is a bit blurred in Fig. 4(a), for  $N = 170000$ , with wider wall. This could have been anticipated from the  $t = 12$  ms profile of the same state in Fig. 2(a). In all cases, after expansion, as the diameter of the cylinder increases, its length has reduced. A study of the diameter and energy of the expanding cylindrical-shell-shaped BEC of  $^{164}\text{Dy}$  atoms of circular section is considered next. In Fig. 5(a) we plot the outer diameter of the expanding hollow cylindrical states of circular section displayed in Fig. 2 versus time  $t$ . In Fig. 5(b) we plot the energy

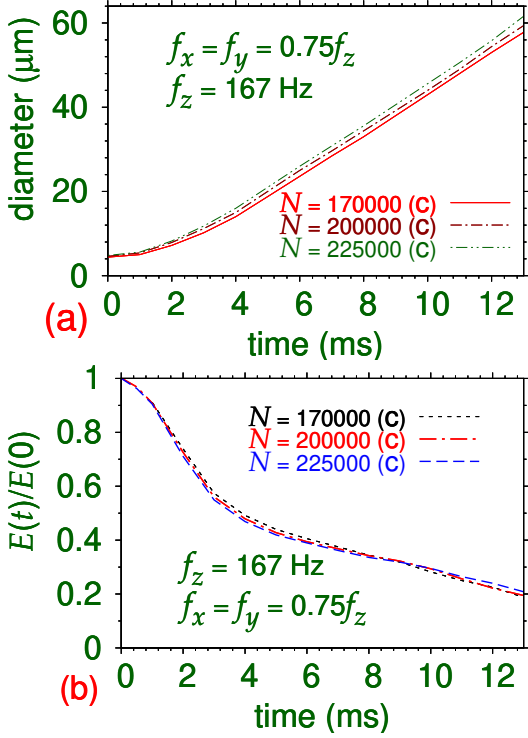


Figure 5: (a) Evolution of the outer diameter in the  $x$ - $y$  plane of the cylindrical-shell-shaped dipolar BEC of  $^{164}\text{Dy}$  atoms with circular section during a quasi-free expansion for different  $N = 170000, 200000,$  and  $225000$ . (b) Evolution of the energy  $E(t)/E(0)$  of the same during this expansion in units of respective energies at  $t = 0$   $E(0)$ : for  $N = 170000$ ,  $E(0)/h = 2193$  Hz; for  $N = 200000$ ,  $E(0)/h = 2368$  Hz; and for  $N = 225000$ ,  $E(0)/h = 2505$  Hz.

(per atom)  $E(t)$  of the same states in unit of the initial  $t = 0$  energy  $E(0)$  versus  $t$ . In Fig. 5(a) the diameter increases monotonically with time, whereas the energy decreases monotonically with time in Fig. 5(b) during expansion. At  $t = 13$  ms the diameter (size) of the expanding state is about  $60 \mu\text{m}$ , large enough for its experimental confirmation. In Fig. 5(b) the evolutions of normalized energy  $E(t)/E(0)$  for  $N = 170000, 200000,$  and  $225000$  are quite similar although the initial energy  $E(0)/h$  of these states are very different.

Finally, we present in Fig. 6 the evolution of the rms size (a)  $\langle x \rangle$  and (b)  $\langle z \rangle$  during the quasi-free expansion of the cylindrical-shell-shaped BEC of  $^{164}\text{Dy}$  atoms of circular section. Not quite unexpected, the rms size  $\langle x \rangle$  has the same behavior as the diameter, viz. Fig. 5(a). In Fig. 6(b) we find that the rms size  $\langle z \rangle$  decreases during expansion but with a periodic oscillation with period  $T_{\text{numeric}} \approx 3.25$  ms. This is because the present expansion is only quasi-free with a trap of frequency

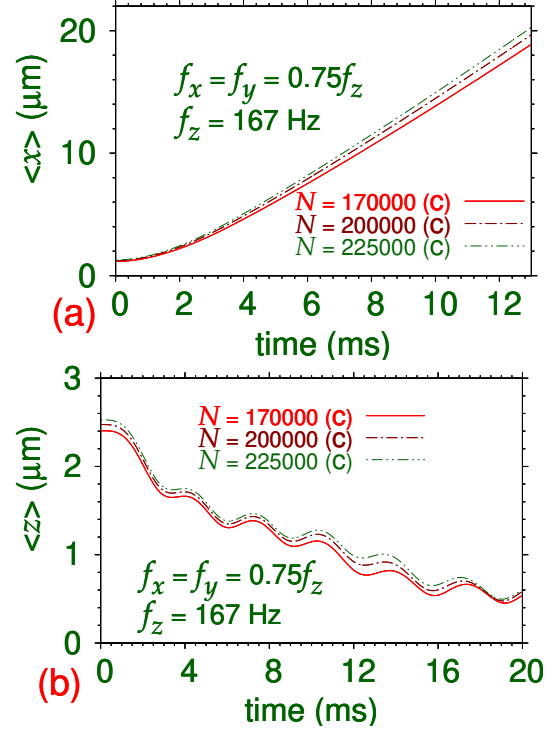


Figure 6: Evolution of the rms size (a)  $\langle x \rangle$  and (b)  $\langle z \rangle$  of the cylindrical-shell-shaped dipolar BEC of  $^{164}\text{Dy}$  atoms with circular section during the quasi-free expansion displayed in Fig. 2 for different  $N = 170000, 200000,$  and  $225000$ .

$f_z = 167$  Hz in the  $z$  direction. Consequently, the expansion dynamics results in a periodic modulation in  $\langle z \rangle$  [54]. This period can be compared with the theoretical period of oscillation of a cylindrically symmetric ( $f_x = f_y$ ) trapped repulsive nondipolar BEC in the hydrodynamic regime [54]

$$f^2 = f_x^2 \left( 2 + \frac{3}{2} \lambda^2 \mp \frac{1}{2} \sqrt{9\lambda^4 - 16\lambda^2 + 16} \right) \quad (12)$$

where  $\lambda = f_z/f_x$ . In the present case of extreme disk-type geometry during the quasi-free expansion  $f_x \rightarrow 0$  and  $\lambda \rightarrow \infty$ , the only surviving frequency is  $\sqrt{3}f_z$ , which corresponds, for  $f_z = 167$  Hz, used in this study, to the period  $T_{\text{theory}} = 1/(\sqrt{3}f_z) \approx 3.54$  ms, in qualitative agreement with the period of  $T_{\text{numeric}} \approx 3.25$  ms found in Fig. 6(b). This agreement is satisfactory considering the fact that the analysis of Ref. [54] considered a repulsive BEC with contact interaction only, whereas the present study has a sizable amount of dipolar attraction and the LHY interaction.

Figures 5 and 6 presents a comprehensive illustration of the expansion dynamics, which is practically insen-

sitive to a variation of the number of atoms. The variation of other parameters – the trapping frequency  $f_z$  and the scattering length  $a$  – are not of much interest from a phenomenological point of view. If the frequency  $f_z$  is reduced the cylindrical-shell-shaped structures disappear; if it is increased the internal radius of the cylinder reduces and for a large enough  $f_z$  the solution is a solid cylinder [13]. We established [13] that for the formation of pronounced shell-shaped solutions one should have  $170 \text{ Hz} > f_z > 140 \text{ Hz}$  and  $f_x \approx f_y = 0.75f_z$ . The scattering length of the dipolar atoms cannot also be varied arbitrarily; we used the value  $a = 80a_0$ . If the scattering length is reduced a bit to  $a = 70a_0$ , the delicate balance between the dipolar attraction and the contact repulsion will be lost and the system will be much too attractive and will collapse. If it is increased a bit to  $a = 90a_0$  the solution has a Gaussian shape. Hence a reasonable variation of the frequency  $f_z$  or of the scattering length  $a$  will destroy the cylindrical-shell-shaped solutions.

#### 4. Summary

In this paper we have studied the expansion dynamics of a high-density dynamically-stable cylindrical-shell-shaped strongly dipolar BEC of  $^{164}\text{Dy}$  atoms [13] for parameters – number of atoms, trap frequencies – quite similar to those employed in recent experiments [8, 52]. We employed an improved mean-field GP model including the LHY interaction [42] appropriately modified for dipolar atoms [43, 45]. We solved the model partial differential equation (8) by real-time propagation and suggest a two-step procedure to carry out the expansion in experiment. We considered a quasi-free expansion of the system radially in the  $x$ - $y$  plane setting the radial trap frequencies  $f_x = f_y = 0$  and maintaining the axial trap frequency  $f_z$  intact. This procedure will allow a radial expansion of the cylindrical-shell-shaped BEC up to a desirable size. The cylindrical shell is found to expand, practically without deformation, over a large period of time. After an expansion during 13 ms, the diameter of the cylindrical shell expands from about  $4 \mu\text{m}$  to  $60 \mu\text{m}$  maintaining the initial symmetry of the cylindrical-shell-shaped state with both circular and elliptic sections. The elliptic symmetry was obtained by introducing a small anisotropy of the trapping potential in the  $x$ - $y$  plane. In all cases studied, as the cylindrical-shell-shaped state expands radially, its axial length contracts a little. During the quasi-free expansion dynamics, the rms size in the polarization  $z$  direction is found to undergo a periodic oscillation controlled by the frequency  $f_z$  of the trap in the  $z$  direction, in accord with a theoretical study [54]. Finally, the  $z$  frequency of the

trap should be reduced slightly to allow the cylinder to expand axially due to dipolar interaction so as to attain the desired size. The steady quasi-free expansion of the cylindrical-shell-shaped strongly dipolar BEC of  $^{164}\text{Dy}$  atoms over a long period of time ensures the possibility of observing such a state in a laboratory in the near future.

#### CRediT authorship contribution statement

L. E. Young-S.: Methodology, Validation, Investigation, Writing – review and editing, Visualization.

S. K. Adhikari: Conceptualization, Methodology, Validation, Investigation, Writing – original draft, Writing – review and editing, Supervision, Funding acquisition, Visualization.

#### Declaration of competing interest

The authors declare that they have no known competing financial interests or personal relationships that could have appeared to influence the work reported in this paper.

#### Data availability

No data was used for the research described in the article.

#### Acknowledgments

LEY-S. would like to acknowledge the financial support by the Vicerrectoría de Investigaciones - Universidad de Cartagena through Project No. 004-2023. SKA acknowledges support by the CNPq (Brazil) grant 301324/2019-0. The use of the supercomputing cluster of the Universidad de Cartagena, Cartagena, Colombia is gratefully acknowledged.

#### References

- [1] J. R. Abo-Shaeer, C. Raman, J. M. Vogels, W. Ketterle, *Science* 292, 476 (2001).
- [2] M. Greiner, O. Mandel, T. Esslinger, T.E. Hänsch, I. Bloch, *Nature (London)* 415, 39 (2002).
- [3] M. Greiner, O. Mandel, T.E. Hänsch, I. Bloch, *Nature (London)* 419, 51 (2002).
- [4] K. E. Strecker, G. B. Partridge, A. G. Truscott, R. G. Hulet, *Nature (London)* 417 (2002) 150.
- [5] L. Khaykovich, F. Schreck, G. Ferrari, T. Bourdel, J. Cubizolles, L. D. Carr, Y. Castin, C. Salomon, *Science* 256 (2002) 1290.
- [6] Y.-J. Lin, K. Jiménez-García, I.B. Spielman, *Nature (London)* 471, 83 (2011).

- [7] H. Kadau, M. Schmitt, M. Wenzel, C. Wink, T. Maier, I. Ferrier-Barbut, T. Pfau, *Nature (London)* 530, 194 (2016).
- [8] M. A. Norcia, C. Politi, L. Klaus, E. Poli, M. Sohmen, M. J. Mark, R. Bisset, L. Santos, F. Ferlaino, *Nature (London)* 596, 357 (2021).
- [9] R. A. Carollo, D. C. Aveline, B. Rhyno, S. Vishveshwara, C. Lannert, J. D. Murphree, E. R. Elliott, J. R. Williams, R. J. Thompson, N. Lundblad, *Nature (London)* 606, 281 (2022).
- [10] D. C. Aveline, J. R. Williams, E. R. Elliott, C. Dutenhoffer, J. R. Kellogg, J. M. Kohel, N. E. Lay, K. Oudrhiri, R. F. Shotwell, N. Yu, R. J. Thompson, *Nature (London)* 582, 193 (2020).
- [11] N. Gaaloul, M. Meister, R. Corgier, A. Pichery, P. Boegel, W. Herr, H. Ahlers, E. Charron, J. R. Williams, R. J. Thompson, W. P. Schleich, E. M. Rasel, N. P. Bigelow, *Nature Commun.* 13, 7889 (2022).
- [12] A. Bassi, L. Cacciapuoti, S. Capozziello, S. Dell’Agnello, E. Diamanti, D. Giulini, L. Iess, P. Jetzer, S. K. Joshi, A. Landragin, C. Le Poncin-Lafitte, E. Rasel, A. Roura, C. Salomon, H. Ulbricht, *npj Microgravity* 8, 49 (2022).
- [13] L. E. Young-S., S. K. Adhikari, *Phys. Rev. A* 108, 053323 (2023).
- [14] A. M. Turner, V. Vitelli, D. R. Nelson, *Rev. Mod. Phys.* 82, 1301 (2010).
- [15] T.-L. Ho, B. Huang, *Phys. Rev. Lett.* 115, 155304 (2015).
- [16] N.-E. Guenther, P. Massignan, A. L. Fetter, *Phys. Rev. A* 96, 063608 (2017).
- [17] S. Moulder, S. Beattie, R. P. Smith, N. Tammuz, Z. Hadzibabic, *Phys. Rev. A* 86, 013629 (2012).
- [18] S. Eckel, J. G. Lee, F. Jendrzejewski, N. Murray, C. W. Clark, C. J. Lobb, W. D. Phillips, M. Edwards, G. K. Campbell, *Nature (London)* 506, 200 (2014).
- [19] M. A. Caracanhas, P. Massignan, A. L. Fetter, *Phys. Rev. A* 105, 023307 (2022).
- [20] M. Z. Hasan, C. L. Kane, *Rev. Mod. Phys.* 82, 3045 (2010).
- [21] X.-L. Qi, S.-C. Zhang, *Rev. Mod. Phys.* 83, 1057 (2011).
- [22] C.-K. Chiu, J. C. Y. Teo, A. P. Schnyder, S. Ryu, *Rev. Mod. Phys.* 88, 035005 (2016).
- [23] N. S. Moller, F. E. A. dos Santos, V. S. Bagnato, A. Pelster, *New J. Phys.* 22, 063059 (2020).
- [24] A. Stern, N. H. Lindner, *Science* 339, 1179 (2013).
- [25] Y. Guo, E. Mercado Gutierrez, D. Rey, T. Badr, A. Perrin, L. Longchambon, V. S. Bagnato, H. Perrin, R. Dubessy, *New J. Phys.* 24, 093040 (2022).
- [26] O. Zobay, B. M. Garraway, *Phys. Rev. Lett.* 86, 1195 (2001).
- [27] O. Zobay, B. M. Garraway, *Phys. Rev. A* 69, 023605 (2004).
- [28] K. Sun, K. Padavić, F. Yang, S. Vishveshwara, C. Lannert, *Phys. Rev. A* 98, 013609 (2018).
- [29] S. K. Adhikari, *Phys. Rev. A* 85, 053631 (2012).
- [30] M. Meister, A. Roura, E. M. Rasel, W. P. Schleich, *New J. Phys.* 21, 013039 (2019).
- [31] A. Tononi, L. Salasnich, *Phys. Rev. Lett.* 123, 160403 (2019).
- [32] T.-L. Ho, V. B. Shenoy, *Phys. Rev. Lett.* 77, 3276 (1996).
- [33] H. Pu, N. P. Bigelow, *Phys. Rev. Lett.* 80, 1130 (1998).
- [34] M. Trippenbach, K. Goral, K. Rzazewski, B. Malomed, Y. B. Band, *J. Phys. B* 33, 4017 (2000).
- [35] K. L. Lee, N. B. Jorgensen, I. Kang Liu, L. Wacker, J. J. Arlt, N. P. Proukakis, *Phys. Rev. A* 94, 013602 (2016).
- [36] A. Wolf, P. Boegel, M. Meister, A. Bala, N. Gaaloul, M. A. Efremov, *Phys. Rev. A* 106, 013309 (2022).
- [37] A. Andriati, L. Brito, L. Tomio, A. Gammal, *Phys. Rev. A* 104, 033318 (2021).
- [38] F. Jia, Z. Huang, L. Qiu, R. Zhou, Y. Yan, D. Wang, *Phys. Rev. Lett.* 129, 243402 (2022).
- [39] A. Tononi, F. Cinti, L. Salasnich, *Phys. Rev. Lett.* 125, 010402 (2020).
- [40] P. Boegel, A. Wolf, M. Meister, M. A. Efremov, *Quantum Sci. Technol.* 8, 034001 (2023).
- [41] B. Rhyno, N. Lundblad, D. C. Aveline, C. Lannert, S. Vishveshwara, *Phys. Rev. A* 104, 063310 (2021).
- [42] T. D. Lee, K. Huang, C. N. Yang, *Phys. Rev.* 106, 1135 (1957).
- [43] A. R. P. Lima, A. Pelster, *Phys. Rev. A* 84, 041604(R) (2011).
- [44] A. R. P. Lima, A. Pelster, *Phys. Rev. A* 86, 063609 (2012).
- [45] R. Schutzhold, M. Uhlmann, Y. Xu, U. R. Fischer, *Int. J. Mod. Phys. B* 20, 3555 (2006).
- [46] H. Kadau, M. Schmitt, M. Wenzel, C. Wink, T. Maier, I. Ferrier-Barbut, T. Pfau, *Nature (London)* 530, 194 (2016).
- [47] M. Schmitt, M. Wenzel, F. Bottcher, I. Ferrier-Barbut, T. Pfau, *Nature (London)* 539, 259 (2016).
- [48] F. Wachtler, L. Santos, *Phys. Rev. A* 93, 061603(R) (2016).
- [49] I. Ferrier-Barbut, H. Kadau, M. Schmitt, M. Wenzel, and T. Pfau, *Phys. Rev. Lett.* 116, 215301 (2016).
- [50] Luis E. Young-S., S. K. Adhikari, *Phys. Rev. A* 105, 033311 (2022).
- [51] J. Hertkorn, J.-N. Schmidt, M. Guo, F. Bottcher, K. S. H. Ng, S. D. Graham, P. Uerlings, T. Langen, M. Zwiernlein, T. Pfau, *Phys. Rev. Research* 3, 033125 (2021).
- [52] L. Chomaz, I. Ferrier-Barbut, F. Ferlaino, B. Laburthe-Tolra, B. L. Lev, T. Pfau, *Rep. Prog. Phys.* 86, 026401 (2023).
- [53] M. Krstajić, P. Juhasz, J. Kuera, L. R. Hofer, G. Lamb, A. L. Marchant, R. P. Smith, *Phys. Rev. A* 108, 063301 (2023).
- [54] S. Stringari, *Phys. Rev. Lett.* 77, 2360 (1996).
- [55] M. Edwards, H. Seddiqi, M. Krygier, B. Benton, C. Clark, Expansion dynamics of a ring Bose-Einstein condensate, *Bull. Am. Phys. Soc.* vol 57, number 1, APS March Meeting Abstracts 2012, H16. 009, <https://meetings.aps.org/Meeting/MAR12/Session/H16.9>.
- [56] M. Nilsson Tengstrand, D. Bohlm, R. Sachdeva, J. Bengtsson, S. M. Reimann, *Phys. Rev. A* 103, 013313 (2021).
- [57] T. Bland, E. Poli, C. Politi, L. Klaus, M. A. Norcia, F. Ferlaino, L. Santos, R. N. Bisset, *Phys. Rev. Lett.* 128, 195302 (2022).
- [58] T. Lahaye, C. Menotti, L. Santos, M. Lewenstein, T. Pfau, *Rep. Prog. Phys.* 72, 126401 (2009).
- [59] R. N. Bisset, R. M. Wilson, D. Baillie, P. B. Blakie, *Phys. Rev. A* 94, 033619 (2016).
- [60] R. Kishor Kumar, L. E. Young-S., D. Vudragović, A. Bala, P. Muruganandam, S. K. Adhikari, *Comput. Phys. Commun.* 195, 117 (2015).
- [61] V. I. Yukalov, *Laser Phys.* 28, 053001 (2018).
- [62] D. B. Karp, J. L. Lpez, *J. Approx. Theory* 218, 42 (2017).
- [63] Luis E. Young-S., S. K. Adhikari, *Commun. Nonlin. Sci. Numer. Simul.* 115, 106792 (2022).
- [64] D. Baillie, P. B. Blakie, *Phys. Rev. Lett.* 121, 195301 (2018).
- [65] Y.-C. Zhang, T. Pohl, F. Maucher, *Phys. Rev. A* 104, 013310 (2021).
- [66] L. E. Young-S., S. K. Adhikari, *Eur. Phys. J. Plus* 137, 1153 (2022).
- [67] E. Poli, T. Bland, C. Politi, L. Klaus, M. A. Norcia, F. Ferlaino, R. N. Bisset, L. Santos, *Phys. Rev. A* 104, 063307 (2021).
- [68] L. E. Young-S., P. Muruganandam, A. Bala, S. K. Adhikari, *Comput. Phys. Commun.* 286, 108669 (2023).
- [69] V. Lonar, L. E. Young-S., S. krbić, P. Muruganandam, S. K. Adhikari, A. Bala, *Comput. Phys. Commun.* 209, 190 (2016).
- [70] P. Muruganandam, S. K. Adhikari, *Comput. Phys. Commun.* 180, 1888 (2009).
- [71] S. Inouye, M. R. Andrews, J. Stenger, H.-J. Miesner, D. M. Stamper-Kurn, W. Ketterle, *Nature (London)* 392, 151 (1998).
- [72] Y. Tang, A. Sykes, N. Q. Burdick, J. L. Bohn, B. L. Lev, *Phys. Rev. A* 92, 022703 (2015).